High-speed method for computing the exact solution for the pressure variations in the nearfield of a baffled piston

J. C. Lockwood and J. G. Willette

Applied Research Laboratories, The University of Texas at Austin, Austin, Texas 78712

(Received 23 March 1972; revised 25 July 1972)

A method is presented whereby the pressure variations at any point in the field of a baffled piston may be efficiently calculated. If a solution for the impulse response of a piston of a given geometry is known, then for harmonic excitation the steady-state field may be computed by evaluating the driving-frequency component of the Fourier transform of the impulse response. This method involves a single integration, whereas the direct numerical solution requires a double numerical integration. An exact, closed-form solution for the impulse response of a rectangular piston is derived. With this solution and the known solution for the impulse response of a circular piston the steady-state solutions for these two geometries are obtained. Three-dimensional and contour plots of data obtained for a circular piston and for a plane of symmetry of a rectangular piston field are presented. The plots for the circular piston compare favorably with previously published plots of data calculated by a double integration.

Subject Classification: 11.2, 11.5, 11.7; 12.7.

INTRODUCTION

The calculation of the pressure distribution in the nearfield of a harmonically excited baffled piston has been the subject of numerous investigations. Recently, the article by Zemanek[1] on the nearfield of a circular piston has generated considerable interest. Zemanek presented three-dimensional and contour plots of pressure data obtained by double numerical integration of the exact integral solution. For the rectangular piston, contour plots of data obtained from an exact solution were published in 1952 by Stenzel.[2] Stenzel reduced the problem to a single integration of a tabulated function (generalized sine and cosine integrals). This integration was then done graphically. Other treatments of the rectangular piston have involved phase approximations. (See, for example, the paper by Freedman.[3])

The purpose of the present paper is to present a method by which the exact pressure distributions may be computed more efficiently than by other exact methods. Both circular and rectangular pistons are treated. We utilize an exact closed-form expression for the response of the pressure field to an impulse acceleration of the piston. By evaluating the Fourier transform of the impulse response at the driving frequency, we obtain the transfer function of the system. This requires only a single numerical integration. The transfer function, when expressed in polar form, gives the amplitude and phase of the pressure variations at a given point. It will be shown that Zemanek's double integration requires more steps than the present method by more than a factor of a/λ, the ratio of piston radius to wavelength. In the case of the rectangular piston Stenzel's graphical integration cannot be used as a high-speed means of calculating the nearfields. A digital computer could be used to perform the integration of the tabulated functions. However, the computation would involve either a double numerical integration or an integration of a complete table of functions. Thus, we feel that owing to its speed and versatility the present method has considerable merit as a means of making nearfield computations.

The use of the impulse response in computing the fields due to arbitrary excitation has been proposed previously, mainly in connection with transient excitations. Oberhettinger,[4] who was the first to derive the impulse response of a circular piston, noted that the response to an arbitrary excitation could be obtained by convolution. Stepanishen,[5] in a series of articles on transients, pointed out that the impulse response of any baffled piston could be obtained by calculating the length of the circular arc on the piston face whose impulse radiation would arrive at each instant of time cophasally at a given field point. He also mentioned that the impulse response could be used to obtain the field for continuous waves. In the case of the rectangular piston Stepanishen apparently regarded the impulse response as a computer problem. We have, however, found a closed-form expression for this response.[6]

In what follows we shall outline our general method for calculating the nearfield. An exact closed-form expression for the impulse response of a rectangular piston will be derived.[7] Plots of the impulse responses of circular and rectangular pistons will be presented and their features discussed. Three-dimensional and contour plots of data for the circular piston and for a plane of symmetry of the rectangular-piston field will be presented. The plots for the circular piston are essentially the same as the corresponding plots published by Zemanek. Finally, we shall discuss our results and compare the number of numerical operations

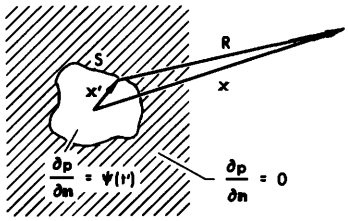

FIG. 1. Geometry of a piston of arbitrary shape in an infinite planar baffle.

required in our solution to the number required in Zemanek's computation.

I. GENERAL THEORY

Our analysis is based on the time-domain Green's-function approach.[8] The pressure field due to a piston occupying a region S of a rigid planar baffle is given by

$$p(\mathbf{x},t) = -\int_{-\infty}^{\infty}\int_{S}\psi(t')\frac{\delta(t-t'-R/c)}{2\pi R}dSdt', \qquad (1)$$
$$R = |\mathbf{x}-\mathbf{x}'|.$$

The geometry is indicated in Fig. 1. Source and field points are designated by primed and unprimed variables, respectively. The function $\psi(t')$ represents the normal derivative of the pressure on the piston face. On the baffle outside S, the normal derivative of the pressure is zero. Equation 1 is a convolution integral. The Fourier transform[9] of the pressure field may be written as a product of the transforms of two time functions, i.e.,

$$P(\mathbf{x},\omega) = -\Psi(\omega)\int_{S}\frac{e^{-j\omega R/c}}{2\pi R}dS. \qquad (2)$$

If we regard Eq. 1 as a linear system with input ψ and output p, the transfer function of the system may be defined as the ratio of the transforms of the output and input functions:

$$H(\mathbf{x},\omega) = \frac{P(\mathbf{x},\omega)}{\Psi(\omega)} = -\int_{S}\frac{e^{-j\omega R/c}}{2\pi R}dS. \qquad (3)$$

Now the transfer function is the Fourier transform of the impulse response $h(\mathbf{x},t)$, which is given by

$$h(\mathbf{x},t) = \mathfrak{F}^{-1}[H(\mathbf{x},\omega)] = -\int_{S}\frac{\delta(t-R/c)}{2\pi R}dS. \qquad (4)$$

For each geometry of interest we wish to evaluate Eq. 1 with the velocity of the piston given as a harmonic function of time, i.e.,

$$v = v_0\cos\omega_0 t = \mathrm{Re}(v_0 e^{j\omega_0 t}). \qquad (5)$$

The momentum equation is used to relate the normal derivative of the pressure to the time derivative of the velocity. We obtain

$$\partial p/\partial \mathbf{n} = \partial p/\partial z = -\rho_0\partial v/\partial t. \qquad (6)$$

On the piston face we have in complex notation

$$\psi(t') = \partial p/\partial \mathbf{n} = -j\omega_0\rho_0 v_0 e^{j\omega_0 t'}. \qquad (7)$$

The Fourier transform of our input function is

$$\Psi(\omega) = -2\pi j\omega_0\rho_0 v_0\delta(\omega-\omega_0). \qquad (8)$$

To obtain the pressure as a complex function of time we must evaluate the inverse transform of $H(\mathbf{x},\omega)\Psi(\omega)$, which may be written

$$p(\mathbf{x},t) = -j\omega_0\rho_0 v_0\int_{-\infty}^{\infty}\delta(\omega-\omega_0)H(\mathbf{x},\omega)e^{j\omega t}d\omega$$
$$= -j\omega_0\rho_0 v_0 H(\mathbf{x},\omega_0)e^{j\omega_0 t}. \qquad (9)$$

Thus, if the impulse response is known, we can solve for the pressure field of a harmonically excited piston by evaluating the Fourier transform of the impulse response. The solution is obtained by the following single integration:

$$p(\mathbf{x},t) = -j\omega_0\rho_0 v_0 e^{j\omega_0 t}\int_{-\infty}^{\infty}h(\mathbf{x},\tau)e^{-j\omega_0\tau}d\tau. \qquad (10)$$

II. IMPULSE RESPONSE

In order to evaluate Eq. 10, we need an expression for the impulse response for the particular geometry of interest. The solution for a circular piston is known and will be stated in a form consistent with the notation of the present authors. Then the impulse response for a rectangular piston will be derived. The impulse response of a circular piston is the solution of Eq. 1 with $\psi(t') = \delta(t')$ and S a circular disk of radius a as shown in Fig. 2. In cylindrical coordinates (ρ,φ,z) Eq. 1 becomes

$$p(\rho,\varphi,z,t) = -\int_{-\infty}^{\infty}\int_{0}^{2\pi}\int_{0}^{a}\delta(t')\frac{\delta(t-t'-R/c)}{2\pi R}\rho'd\rho'd\varphi'dt',$$

with

$$R = [z^2+\rho^2+\rho'^2-2\rho\rho'\cos(\varphi-\varphi')]^{\frac{1}{2}}. \qquad (11)$$

The result, which was first obtained by Oberhettinger,[10] is as follows:

If $\rho<a$,

$$(1/c)h(\mathbf{x},t) = \begin{cases} 0, & t<t_1, \\ 1, & t_1<t<t_2, \\ \frac{1}{\pi}\cos^{-1}\left\{\dfrac{c^2t^2-z^2+\rho^2-a^2}{2\rho(c^2t^2-z^2)^{\frac{1}{2}}}\right\}, & t_2<t<t_3, \\ 0, & t_3<t, \end{cases} \qquad (12)$$

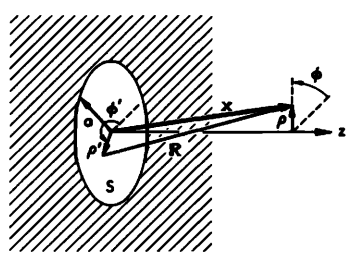

FIG. 2. Geometry of a circular piston in an infinite planar baffle.

If $\rho > a$,

$$(1/c)h(\mathbf{x},t) = \begin{cases} 0, & t<t_2, \\ \frac{1}{\pi}\cos^{-1}\left\{\dfrac{c^2t^2-z^2+\rho^2-a^2}{2\rho(c^2t^2-z^2)^{\frac{1}{2}}}\right\}, & t_2<t<t_3, \\ 0, & t_3<t. \end{cases} \quad (13)$$

The limits are given by

$$\begin{aligned} t_1 &= z/c, \\ t_2 &= (1/c)[z^2+(\rho-a)^2]^{\frac{1}{2}}, \\ t_3 &= (1/c)[z^2+(\rho+a)^2]^{\frac{1}{2}}. \end{aligned} \quad (14)$$

These limits correspond to the travel times of signals arriving at the field point from the nearest point (for $\rho<a$), the nearest edge, and the farthest edge of the piston, respectively. Figure 3 gives some typical time plots of Eqs. 12 and 13 for various values of ρ. Note that to obtain the pressure field for harmonic excitation from Eq. 10, the integral need be carried out only for the range of time for which $h(\mathbf{x},t)$ is nonzero. Moreover, for $\rho<a$, the integral for the range of time during which $h(\mathbf{x},t)$ is constant may be evaluated

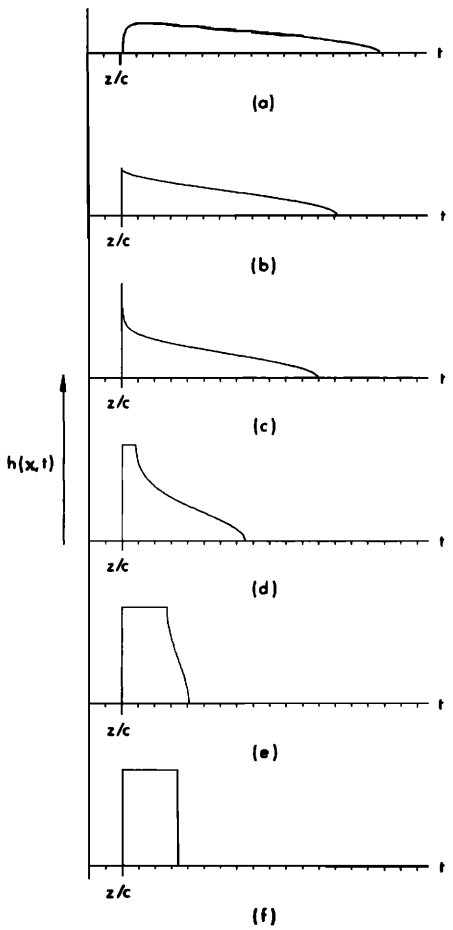

FIG. 3. Impulse response of a circular piston for $z/a=5.0$, (a) $\rho/a=1.2$, (b) $\rho/a=1.0$, (c) $\rho/a=0.9$, (d) $\rho/a=0.5$, (e) $\rho/a=0.1$, (f) $\rho/a=0.0$. (Note: The vertical axis is not located at $t=0$.)

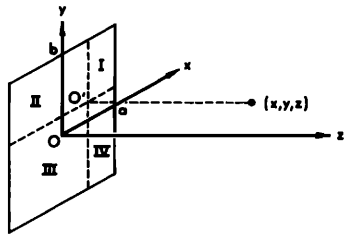

FIG. 4. Geometry of a rectangular piston. The rectangle is subdivided into four rectangles and the sum of the individual fields in front of the common corner point evaluated.

analytically. The range from t_2 to t_3 is integrated numerically.

Some features of the curves in Fig. 3 are worth noting. Curve (a) corresponds to a point outside the geometrical beam and begins with zero amplitude at the time of first arrival. Curve (b) corresponds to a point on the edge of the beam and begins with half amplitude. Curve (c) is for a point close to the edge of the beam and begins with full amplitude but quickly drops to half amplitude and then drops more slowly. The numerical integration for points that have an impulse response like Fig. 3(c) must be done carefully because the impulse response may contain important frequency components much higher than the driving frequency and a larger number of samples may be required in the vicinity of t_2 than on the more well-behaved parts of the curve. The subsequent curves show that the time between t_2 and t_3 becomes progressively smaller as ρ is decreased until in the vicinity of $\rho=0$ the function approaches a step.

The impulse response for a rectangular piston is somewhat more complicated than that for a circular piston. Our derivation for the rectangular piston is by a method similar to that used by Farn and Huang[11] to obtain the same solution that Oberhettinger had obtained for transient radiation from a piston. Consider a rectangular piston of length 2b and width 2a as shown in Fig. 4. For any field point (x,y,z) we locate its projection $O'=(x,y,0)$ on the plane of the piston. Four rectangles are defined, each with a corner at O', such that by combining the fields of the four rectangles the field of the original piston is obtained.[12] If O' is outside the original rectangle, the rectangle is enlarged to include it and the added rectangles are subtracted. We now solve for the field at a point whose projection lies on the corner of a rectangle. Let the longer and shorter sides be denoted by l and s, respectively, as shown in Fig. 5. Equation 1 is written in cylindrical coordinates with origin at the corner. Following the time integration we have

$$\begin{aligned} p(0,0,z,t) = -\Bigg[&\int_0^s \int_0^{\pi/2} \frac{\delta(t-R/c)}{2\pi R} d\varphi' \rho' d\rho' \\ &+ \int_s^l \int_{\cos^{-1}s/\rho'}^{\pi/2} \frac{\delta(t-R/c)}{2\pi R} d\varphi' \rho' d\rho' \\ &+ \int_l^{(l^2+s^2)^{\frac{1}{2}}} \int_{\cos^{-1}s/\rho'}^{\pi/2-\cos^{-1}l/\rho'} \frac{\delta(t-R/c)}{2\pi R} d\varphi' \rho' d\rho' \Bigg]. \end{aligned} \quad (15)$$

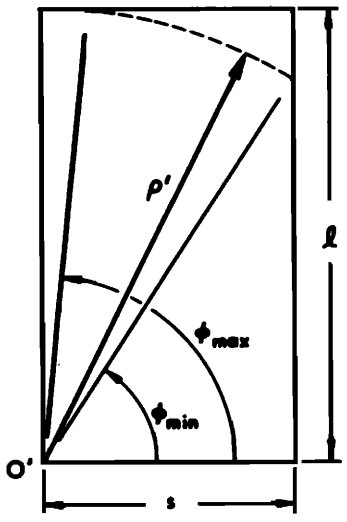

FIG. 5. Geometry for evaluation of the impulse response of a rectangle at a point in front of a corner.

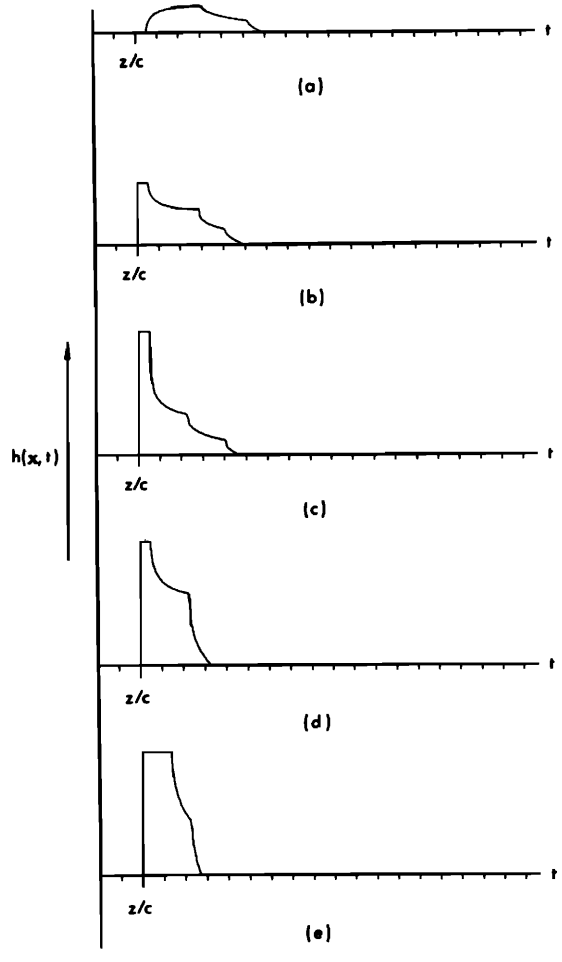

FIG. 6. Impulse response of a rectangular piston for $z/a=10.0$ and $b/a=1.5$. (a) $x/a=1.4$, $y/b=1.25$; (b) $x/a=1.0$, $y/b=0.75$; (c) $x/a=0.6$, $y/b=0.75$; (d) $x/a=0.6$, $y/b=0.0$; (e) $x/a=0.0$, $y/b=0.0$. (Note: The vertical axis is not located at $t=0$.)

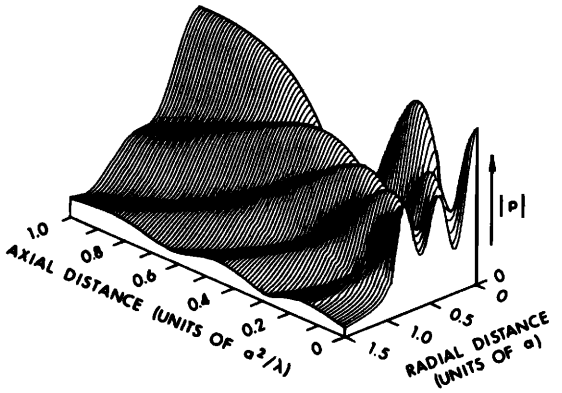

FIG. 7. Three-dimensional plot of pressure amplitude in the nearfield of a circular piston ($a/\lambda=2.5$).

Since the origin has been chosen so that the field point is on the axis, we have $R=(z^2+\rho'^2)^{\frac{1}{2}}$. The φ' integration is trivial and the ρ' integration is effected by the sifting property of the δ function following the change of variables $\tau=t-R/c$. It is convenient to leave the final integration over a δ function undone. The result is written

$$p(0,0,z,t)=-\frac{c}{2\pi}\left\{\int_{\tau_1}^{\tau_4}\frac{\pi}{2}\delta(\tau)d\tau-\int_{\tau_2}^{\tau_4}\cos^{-1}\left\{\frac{s}{[c^2(t-\tau)^2-z^2]^{\frac{1}{2}}}\right\}\delta(\tau)d\tau-\int_{\tau_3}^{\tau_4}\cos^{-1}\left\{\frac{l}{[c^2(t-\tau)^2-z^2]^{\frac{1}{2}}}\right\}\delta(\tau)d\tau\right\},$$

where

$$\begin{aligned}\tau_1&=t-z/c,\\ \tau_2&=t-(1/c)(z^2+s^2)^{\frac{1}{2}},\\ \tau_3&=t-(1/c)(z^2+l^2)^{\frac{1}{2}},\\ \tau_4&=t-(1/c)(z^2+s^2+l^2)^{\frac{1}{2}}.\end{aligned}\tag{16}$$

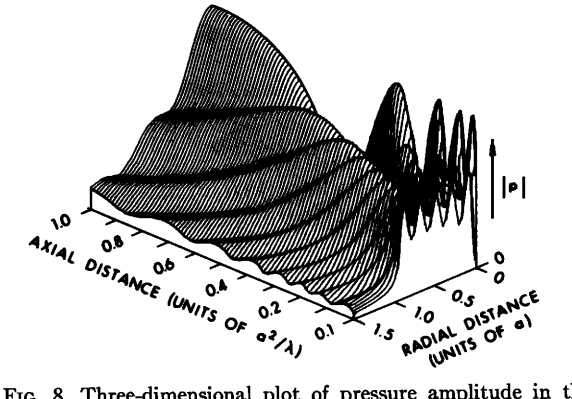

FIG. 8. Three-dimensional plot of pressure amplitude in the nearfield of a circular piston ($a/\lambda=5.0$).

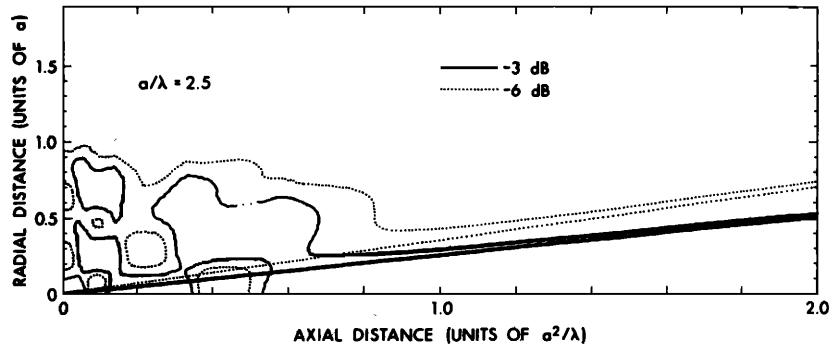

FIG. 9. Contour plot of relative pressure amplitude in the nearfiled of a circular piston ($a/\lambda=2.5$).

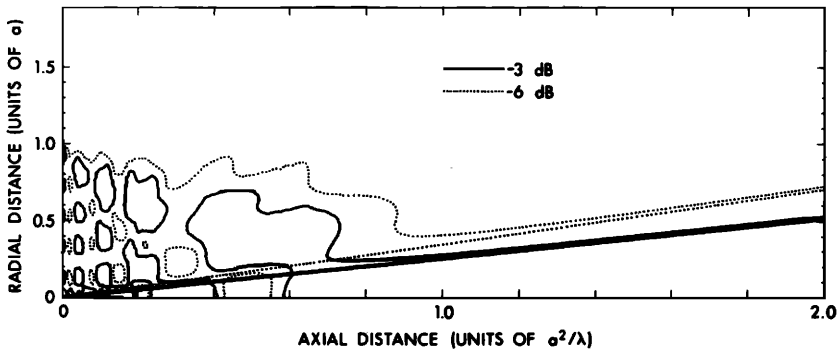

FIG. 10. Contour plot of relative pressure amplitude in the nearfield of a circular piston ($a/\lambda=5.0$).

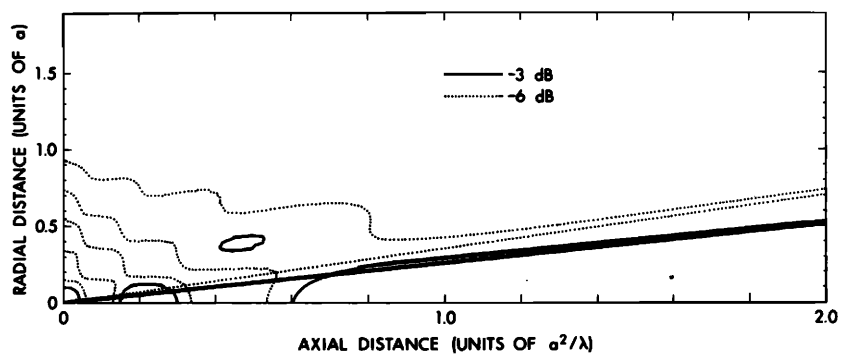

FIG. 11. Contour plot of pressure amplitude in the nearfield of a circular picton ($a/\lambda=2.5$.)

The integrals are evaluated by inspection, since

$$\int_{\tau_1}^{\tau_2} f(\tau)\delta(\tau)d\tau = f(0), \quad \text{if} \quad \tau_1 \leqq \tau \leqq \tau_2, \qquad = 0, \quad \text{otherwise.} \tag{17}$$

The exact solution for the impulse response of the rectangular piston for an arbitrary field point is obtained by superposition and may be written

$$h(\mathbf{x},t) = -\frac{c}{2\pi}\sum_{i=1}^{4} \pm\left\{\int_{\tau_{1i}}^{\tau_{4i}} \frac{\pi}{2}\delta(\tau)d\tau - \int_{\tau_{2i}}^{\tau_{4i}} \cos^{-1}\left\{\frac{s_i}{[c^2(t-\tau)^2-z^2]^{\frac{1}{2}}}\right\}\delta(\tau)d\tau - \int_{\tau_{3i}}^{\tau_{4i}} \cos^{-1}\left\{\frac{l_i}{[c^2(t-\tau)^2-z^2]^{\frac{1}{2}}}\right\}\delta(\tau)d\tau\right\},$$

where

$$\begin{aligned} \tau_{1i} &= t - z/c, \\ \tau_{2i} &= t - (1/c)(z^2+s_i^2)^{\frac{1}{2}}, \\ \tau_{3i} &= t - (1/c)(z^2+l_i^2)^{\frac{1}{2}}, \\ \tau_{4i} &= t - (1/c)(z^2+s_i^2+l_i^2)^{\frac{1}{2}}. \end{aligned} \tag{18}$$

The lengths of the short and long sides of the ith rectangle, s_i and l_i, as well as whether the ith contribution is to be added or subtracted, are to be determined by logic. Figure 6 gives plots of Eq. 18 for several field-point locations. The function $h(\mathbf{x},t)$ is proportional to the length of the arc on the piston face whose impulse radiation would arrive at the field point at time t. The discontinuities in slope occur at times when the active arc suddenly attains a different rate of change due to its intersection with one or more sides. Note that, as in the case of the circular piston, curve a, which corresponds to a point outside the geometrical beam,

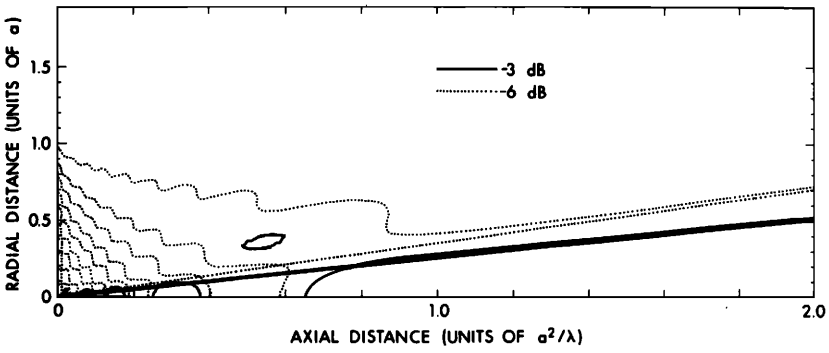

FIG. 12. Contour plot of pressure amplitude in the nearfield of a circular piston ($a/\lambda=5.0$).

begins with zero amplitude at the first arrival, curve b, corresponding to a point on the edge of the beam, begins with half amplitude at the first arrival, and the subsequent curves, for points within the beam, begin with full amplitude.

III. RESULTS

In this section, plots of data obtained by the present method are presented. The data for the circular piston were computed for $a/\lambda=2.5$ and $a/\lambda=5.0$ so that a qualitative check against Zemanek's results would be possible. Figures 7 and 8 are plots corresponding to Figs. 5 and 6 of Ref. 1 for $a/\lambda=2.5$ and $a/\lambda=5.0$, respectively. The similarity of our plots to those of Zemanek leaves little doubt that our solution gives similar results. Figures 9 and 10 are contour plots corresponding to Figs. 8(a) and 9(a) of Ref. 1. The straight line that begins at the origin and eventually merges with the -3-dB contour in the farfield was computed from the farfield directivity factor [Eq. (5) of Ref. 1]. In comparing Figs. 9 and 10 with the corresponding plots of Ref. 1, we find that there is a slight discrepancy in the location where the farfield contours obtained from the numerical solution become coincident with the farfield contours computed from the directivity factor. We cannot explain this discrepancy; however, the two numerical solutions appear to be in good agreement.

While Figs. 9 and 10 give a good picture of the radial variations to be expected at any range, they are slightly misleading for visualizing the pressure variations within the nearfield as a whole. The reason is that they are referred to the maximum pressure at each range. (Zemanek calls these plots of relative pressure.) Figures 11 and 12 are contours for $a/\lambda=2.5$ and $a/\lambda=5.0$ referenced to the maximum of the axial variations from $z=0.0$ to $z=a^2/\lambda$. Beyond $z=a^2/\lambda$ the axial value is the maximum for each range and the reference is the axial value. These contours delineate the features shown in the three-dimensional plots (Figs. 7 and 8).

We are including only two plots of data obtained from our solution for the nearfield of a rectangular piston. Figure 13 is a three-dimensional plot of pressure amplitude in the x–z plane for $y=0$. The plot is for $a/\lambda=2.5$, where $2a$ is the x extent of the piston. The aspect ratio b/a is 1.5. The plot shows the expected absence of strong peaks and nulls in the nearfield of a rectangular piston. This absence of strong interference patterns can be inferred from the shape of the impulse response. If one imagines the convolution of the impulse response with a sinusoid, he can see that in order for the signal resulting from the end of the impulse response to interfere strongly with the one resulting from the beginning, the impulse response must have an abrupt drop at the end as does the axial impulse response for a circular piston. Since the impulse response of a rectangular piston always is spread out at the end, strong interference in the nearfield is impossible. Figure 14 is a contour plot of pressure amplitude in the x–z plane of a rectangular piston. The piston dimensions are those used for Fig. 13. The axial maximum, which occurs for this case at axial distance $z=2.4a^2/\lambda$, was used as the reference value from $z=0.0$ to $z=2.4a^2/\lambda$. Beyond $z=2.4a^2/\lambda$ the axial value was used as the reference.

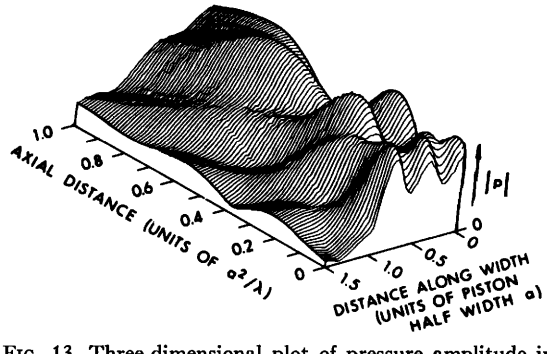

FIG. 13. Three-dimensional plot of pressure amplitude in the x-z plane of a rectangular piston field ($a/\lambda=2.5$, $b/a=1.5$).

IV. EVALUATION OF THE TECHNIQUE

As was mentioned in the Introduction, the primary purpose of this paper is to present a high-speed method of calculating nearfield data. Zemanek, in Ref. 1, indicates the number of elemental areas whose contributions must be summed to give convergent results for a given wavelength and piston radius. We are, therefore, able to make a quantitative estimate of the relative

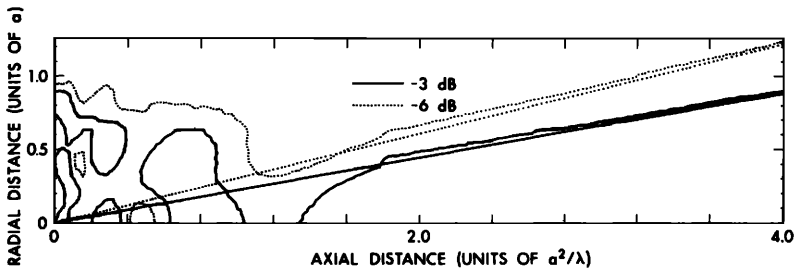

FIG. 14. Contour plot of pressure amplitude in the x-z plane of a rectangular piston field ($a/\lambda=2.5$, $b/a=1.5$).

speeds of our method and that of Zemanek. The number of contributions summed by Zemanek is $16\pi a^2/\lambda^2$. In the present method we numerically integrate the product of the impulse response with a cosine and a sine function oscillating at the driving frequency to obtain the real and imaginary parts of the pressure. The number of steps required in the integration depends on the length of the nonconstant part of the impulse response and on the driving frequency. We have found that convergent results are obtained if we sample the function 10 times per cycle of the driving frequency, with the proviso that at least 20 increments be used. The maximum length of the nonconstant part of the impulse response is $2a/c$ so that an upper bound on the number of calculations used in the present method is $10f\cdot 2a/c=20a/\lambda$, except when that number is less than 20. (f and c are the frequency in hertz and the sound speed, respectively.) The stated sampling rate is adequate except when ρ is only slightly less than a. In that case, as was pointed out previously, there is a very large slope following the beginning of the impulse response. We therefore break up the beginning of the integration into 10 smaller increments for values of ρ close to a. This does not have an appreciable effect on the overall speed of the method. Moreover, for most points the part of the impulse response that must be integrated is shorter than $20a/\lambda$; so, our stated upper bound is still an overestimate. It is thus apparent that the speed of our method is proportional to a/λ, whereas the speed of the direct numerical integration is proportional to $(a/\lambda)^2$.

V. SUMMARY

A method has been outlined whereby the pressure in the nearfield of a harmonically excited piston may be computed from the exact theory more efficiently than by previous methods. The computation involves a numerical integration of the impulse response multiplied by an exponential function oscillating at the driving frequency. An exact closed-form solution for the impulse response of a rectangular piston was derived. Plots of data for a circular piston were presented for comparison with those published by Zemanek. The agreement is excellent. As an example of the application of the method for calculating the nearfield of a rectangular piston, a three-dimensional and a contour plot of pressure on one plane of symmetry of a rectangular piston were presented. The plots show the absence of the strong interference peaks and nulls that characterize the nearfield of a circular piston.

ACKNOWLEDGMENTS

The authors gratefully acknowledge many helpful discussions with Dr. H. O. Berktay. This work was supported by the Office of Naval Research.

[1]J. Zemanek, "Beam Behavior within the Nearfield of a Vibrating Piston," J. Acoust. Soc. Am. **49,** 181 (1971).
[2]H. Stenzel, "Die akustische Strahlung der recteckigen Kolbenmembran," Acustica **2,** 263 (1952).
[3]A. Freedman, "Sound Field of a Rectangular Piston," J. Acoust. Soc. Am. **32,** 197 (1960).
[4]F. Oberhettinger, "On Transient Solutions of the Baffled Piston Problem," J. Res. Natl. Bur. Stand. (U.S.) B **65,** 1 (1961).
[5]P. R. Stepanishen, J. Acoust. Soc. Am. **49,** 283 (1971); J. Acoust. Soc. Am. **49,** 841 (1971); J. Acoust. Soc. Am. **49,** 1629 (1971).
[6]Stepanishen (private communication) has recently obtained an exact form of the impulse response for the rectangular piston. A single term was obtained; however, its form is dependent on the location of the field point.
[7]This solution was developed by one of the authors (JCL) in collaboration with H. O. Berktay and was the subject of a paper presented at the 83rd Meeting of the Acoustical Society of America, Buffalo, New York (April 1972) [J. Acoust. Soc. Am. **52,** 154 (1972)].
[8]P. M. Morse and K. U. Ingard, *Theoretical Acoustics* (McGraw-Hill, New York, 1968).
[9]The Fourier transform notation in this paper is consistent with that in B. P. Lathi, *Communication Systems* (Wiley, New York, 1968).
[10]See Ref. 4. Oberhettinger derives this result from King's integral, which is also a single-integral representation of the exact solution for the circular-piston case. We believe that Eq. 10 is more amenable to fast numerical integration than is King's integral. Moreover, the rectangular piston and other geometries can be treated by the present method.
[11]C. L. S. Farn and H. Huang, "Transient Acoustic Fields Generated by a Body of Arbitrary Shape," J. Acoust. Soc. Am. **43,** 252 (1968).
[12]This method of evaluating the field of a rectangle by breaking it up into four rectangles and evaluating the field of each in front of a corner was used by Stenzel, Ref. 2.